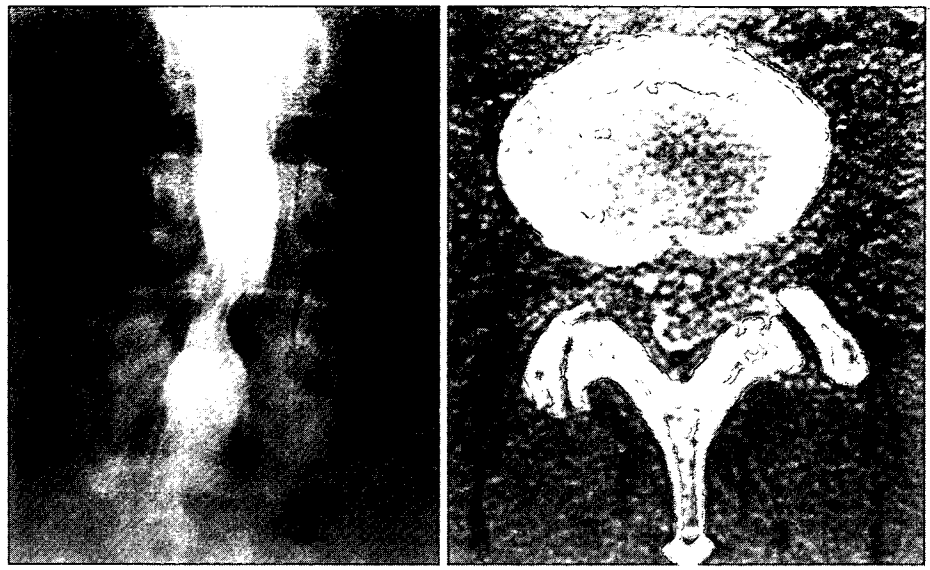

FIG. 3. Lumbar myelogram *(left)* and axial computed tomography scan *(right)* revealing marked stenosis bilaterally at the L4–5 disc space with an extradural filling defect.

rological deficit. A postoperative MR imaging examination revealed a decompressed dural sac with no extradural mass (Fig. 6).

Discussion

Rheumatoid nodules, one of the components of the American Rheumatism Association classification criteria for RA, produce extraarticular symptoms. Rheumatoid nodules often occur in regions subject to mechanical stimulation, such as the elbow, forearm, wrist, knee, occipital region, and certain other locations. They rarely occur in the pleura, lungs, pericardium, heart, intestine, or meninges.[5] Direct involvement of the brain, spinal cord, or meninges by rheumatoid nodules is rare.[4] There have been few reports of extradural rheumatoid nodules; to our knowledge, there are only four cases in the literature.[8,12,16] In two cases these nodules arose in the thoracic region, and in two cases they were in the lumbar region. In our patient, the rheumatoid nodules were found in the extradural space of the lumbar region at the level of L4–5, which may receive the most mechanical stress in the lumbar region.[13] Our patient had no

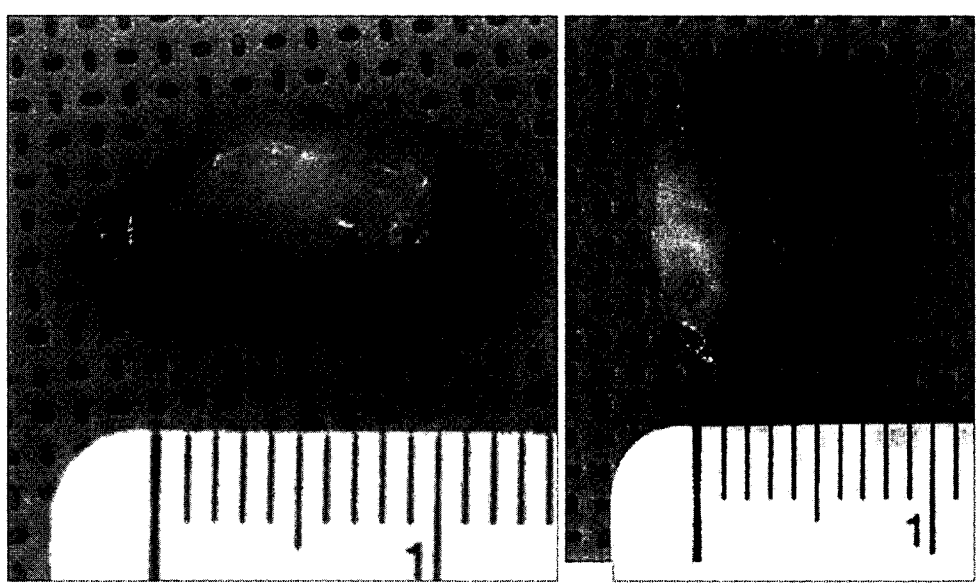

FIG. 4. Gross appearance of the extradural rheumatoid nodules removed. The nodules were covered with a yellow membrane, and one of them measured 1.2 × 0.7 × 0.7 cm.

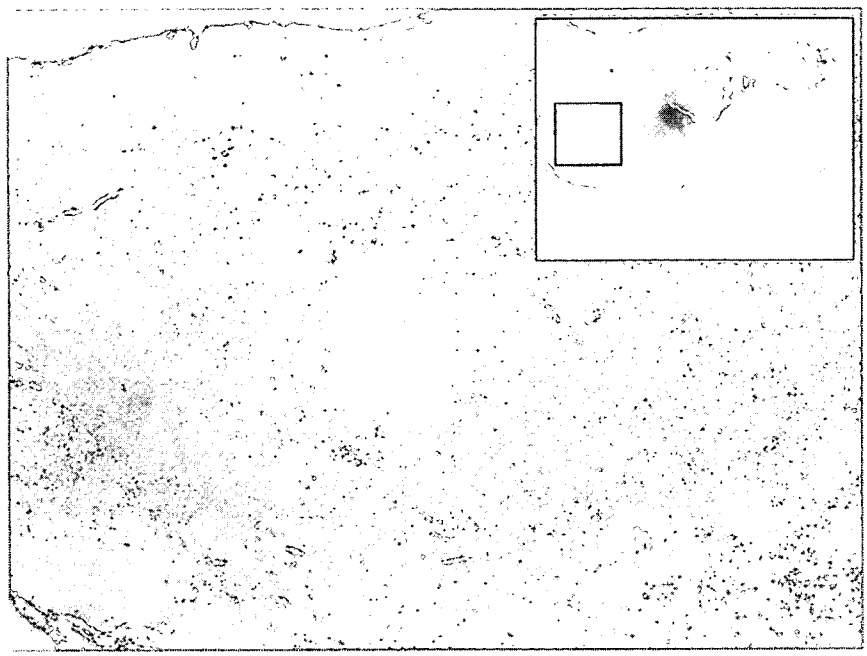

FIG. 5. Photomicrographs of lesion sections demonstrating extensive areas of fibrinoid necrosis surrounded in some parts with poorly formed palisades of histiocytes and chronic inflammatory cells. The *black box* indicates the area of magnification in the larger image. H & E, original magnifications × 100 and × 20 *(inset)*.

clinical instability at L4–5. We removed the nodules via partial laminectomy using a microscope for the minimally invasive procedure, and as a result were able to preserve the posterior elements of the lumbar spine. At the most recent follow-up examination, there was no recurrence. If the nodules recur in the future, we will perform an additional surgery such as lumbar spinal fusion.

Generally, laboratory studies in patients with rheumatoid nodules tend to reveal an elevated RF level.[1,9] In our patient the RF level was elevated (265 U/ml), but the C-reactive

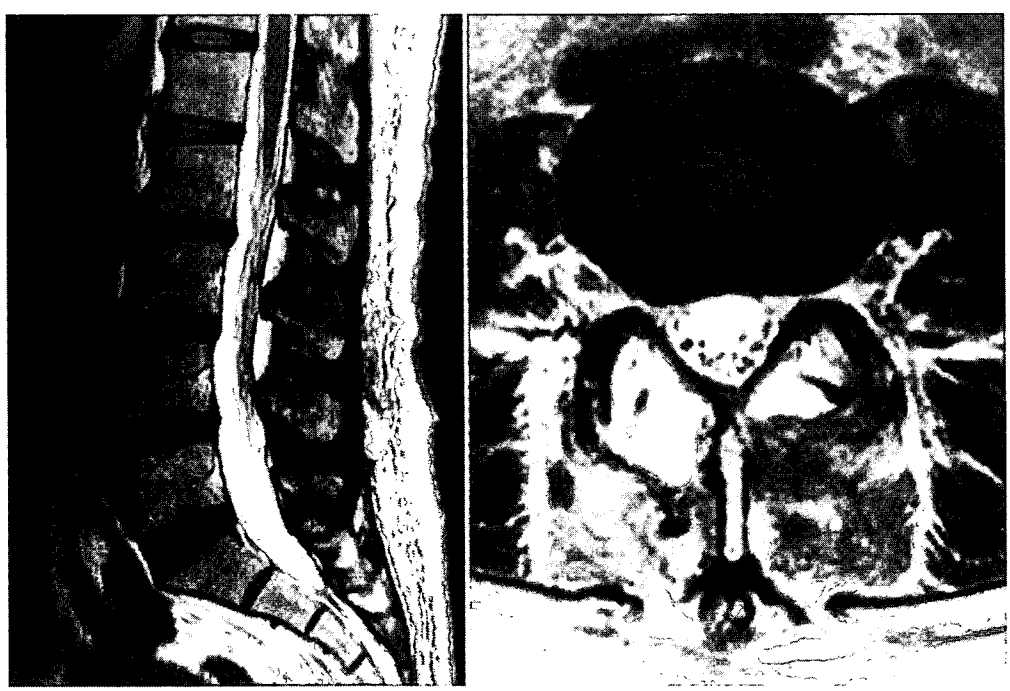

FIG. 6. Postoperative T2-weighted sagittal *(left)* and axial *(right)* MR images showing complete removal of the masses and no compression of the dura mater.

protein level was almost within normal limits (0.45 mg/dl) and was successfully controlled with pharmacotherapy.

If patients with RA complain of leg pain, attention is usually given to major joints such as the hips and knees. In our case, the lesion was successfully detected on MR imaging of the lumbar spine. Without MR imaging of the lumbar spine, we might have overlooked this lesion. The differential diagnosis of extradural rheumatoid nodules in the lumbar region includes juxtafacet cysts, facet cysts, ligamentum flavum cysts, nerve sheath tumors, and hematomas. Although involvement of the cervical spine in RA has often been reported, there have been few reports on thoracic and lumbar spine involvement in patients with RA.[1-3,10,11,14] Heywood and Meyers[3] reported that the incidence of patients with symptomatic subcervical RA was 0.94%, while that of patients with neurological symptoms due to this condition was 0.25%. Lawrence and colleagues[7] found that the morbidity rate in patients with RA and associated lumbar vertebral lesions was 5% for men and 3% for women. However, in the radiological investigation of lumbar lesions in 224 patients with RA conducted by Kuwahara et al.,[6] there were pathological changes in 143 patients (63.8%). Patients tended to complain of symptoms less often than changes were revealed on imaging. We suspect that there are few reported lumbar spine symptoms in patients with RA because the daily life activities of these patients are limited and because symptoms are believed to arise from lesions in the major joints of the legs. Thus, MR imaging examination is important for detection of lumbar lesions in patients with RA. Tajima and colleagues[15] reported that MR imaging could detect rheumatoid nodular changes, slight compression fractures, and erosion of vertebral bodies, and permit quantitative determination of the severity of intervertebral disc degeneration.

Although the incidence of extraarticular lesions of the lumbar spine differ among the reports in the literature, there are characteristic lesions of RA in the lumbar spine as well as the cervical spine, and attention should thus be paid to lumbar spine symptoms.

Conclusions

We have reported on a rare case of symptomatic rheumatoid nodules in the lumbar extradural region that compressed the L-5 nerve roots bilaterally. Magnetic resonance imaging is essential in the detection of such lesions in patients with RA.

References

1. Baggenstoss AH, Bickel WH, Ward LE: Rheumatoid granulomatous nodules as destructive lesions of vertebrae. **J Bone Joint Surg Am 34:**601–609, 1952
2. Friedman H: Intraspinal rheumatoid nodule causing nerve root compression. **J Neurosurg 32:**689–691, 1970
3. Heywood AW, Meyers OL: Rheumatoid arthritis of the thoracic and lumbar spine. **J Bone Joint Surg Br 68:**362–368, 1986
4. Jackson CG, Chess RL, Ward JR: A case of rheumatoid nodule formation within the CNS and a review of the literature. **J Rheumatol 11:**237–240, 1984
5. Kersley GD, Ross FG, Fowles SJ, Johnson C: Tomography in arthritis of the small joints. **Ann Rheum Dis 23:**280, 1964
6. Kuwahara S, Kimura C, Tajima N, Aso K, Sugano T: Radiological findings of the lumbar spine in rheumatoid arthritis. **Jpn J Rheum 2:**13–24, 1989
7. Lawrence JS, Sharp J, Ball J, Bier F: Rheumatoid arthritis of the lumbar spine. **Ann Rheum Dis 23:**205–217, 1964
8. Linquist PR, McDonnell DE: Rheumatoid cyst causing extradural compression. A case report. **J Bone Joint Surg Am 52:** 1235–1240, 1970
9. Lorber A, Pearson CM, Rene RM: Osteolytic vertebral lesions as a manifestation of rheumatoid arthritis and related disorders. **Arthritis Rheum 4:**514–532, 1961
10. Magnaes B, Hauge T: Rheumatoid arthritis contributing to lumbar spinal stenosis. Neurogenic intermittent claudication. **Scand J Rheumatol 7:**215–218, 1978
11. Nakase T, Fujiwara K, Kohno J, Owaki H, Tomita T, Yonenobu K, et al: Pathological fracture of a lumbar vertebra caused by rheumatoid arthritis—a case report. **Int Orthop 22:**397–399, 1998
12. Richard I, Jones AW: Rheumatoid nodule formation within the lumbar extradural space. **J Neurol Neurosurg Psychiatry 52:** 414, 1989
13. Sairyo K, BiyaniA, Goel V, Leadman D, Booth R Jr, Ebraheim N, et al: Pathomechanism of ligamentum flavum hypertrophy: a multidisciplinary investigation based on clinical, biomechanical, histologic, and biologic assessments. **Spine 30:**2649–2656, 2005
14. Shichikawa K, Matsui K, Oze K, Ota H: Rheumatoid spondylitis. **Int Orthop 2:**53–60, 1978
15. Tajima N, Tashiro K, Saisho K, Kimura C, Suzuki Y: Magnetic resonance imaging of the lumbar spine in rheumatoid arthritis. **Jpn J Rheum Joint Surg 7:**321–328, 1988
16. Tsegaye M, Bassi S, Ashpole RD: Extradural spinal cord compression by rheumatoid nodule. **Br J Neurosurg 17:**255–257, 2003

Manuscript submitted March 28, 2007.
Accepted May 23, 2007.

Address reprint requests to: Natsuo Yasui, M.D., 3-18-15 Kuramoto-cho, Tokushima 770-8503, Japan. email: nyasui@clin.med.tokushima-u.ac.jp.

ORIGINAL

Unilateral chronic insufficiency of anterior cruciate ligament decreases bone mineral content and lean mass of the injured lower extremity

Shinjiro Takata, Aziz Abbaspour, Michiharu Kashihara, Shigetaka Nakao, and Natsuo Yasui

Department of Orthopedics, Institute of Health Bioscieces, The University of Tokushima Graduate School, Tokushima, Japan

Abstract : We studied the effects of unilateral chronic anterior cruciate ligament (ACL) injury on bone size, bone mineral content (BMC), bone mineral density (BMD), soft tissue composition and muscle strength of the injured lower extremity in Japanese 21 men and 12 women aged 15 to 39 years. Bone area, BMD, BMC, lean mass and fat mass of lower extremity were measured using dual energy X-ray absorptiometry. The isometric and isokinetic muscle strength was assessed by an isokinetic machine.

BMC, lean mass, circumference of the thigh and circumference of the lower leg of the injured lower extremity were significantly smaller than those of the intact lower extremity ($p=0.0002$, $p<0.0001$, $p<0.0001$, $p=0.0131$). In cotrast, fat mass and %Fat of the injured lower extremity was significantly greater than that of the intact lower extremity ($p=0.0301$, $p<0.0001$). Bone area and BMD did not produce significant difference. These findings suggest that chronic insufficiency of ACL decreases BMC and lean mass of the injured lower extremity. J. Med. Invest. 54 : 316-321, August, 2007

Keywords **:** *anterior cruciate ligament injury, bone area, bone mineral content, bone mineral density, dual energy X-ray absorptiometry*

INTRODUCTION

ACL injury is a common knee trauma in sports, and it often causes chronic symptomatic instability (1) and proprioceptive deficit of the knee on the injured side (2). Chronic instability of the knee joint resulting from ACL injury induces muscle atrophy (3, 4), muscle weakness (2, 5), and degenerative changes of the knee joint (1), and bone atrophy of the leg on the injured side (6, 7).

Received for publication June 15, 2007 ; accepted July 4, 2007.

Address correspondence and reprint requests to Shinjiro Takata, M.D., Ph.D., Department of Orthopedics, Institute of Health Biosciences, The University of Tokushima Graduate School, Kuramoto-cho, Tokushima 770-8503, Japan and Fax : +81-88-633-0178.

Mechanical stress is an important determinant to prevent musculoskeletal atrophy of the lower extremity. Therefore, reduction of mechanical stress on the legs in patients with unilateral ACL injury may lead to diminution of the synthesis of contractile protein and bone formation, which may result in disuse musculoskeletal atrophy of the lower extremity on the injured side. Hence, early and vigorous rehabilitation is required to prevent disuse musculoskeletal atrophy of the lower extremity, so that patients with ACL injury can return to sports as early as possible (8, 9).

The purpose of this study was to clarify the effects of unilateral ACL injury on bone area, BMC, BMD and soft tissue composition of lower extremity. The question of whether chronic ACL injury de-

creases bone size of the injured lower extremity or not has not been adequately solved.

MATERIALS AND METHODS

Twenty-one men and twelve women with unilateral untreated ACL injury, whose age ranged from 15 to 39 years were studied. Table 1 showed characteristics of men and women with unilateral untreated ACL injury. In all patients, pivot-shift and Lachman's test were positive. Thirty-two of 33 patients underwent ACL reconstruction surgery with a central third patellar tendon graft (bone-patellar tendon-bone graft) (10).

All subjects agreed to participate in this study and gave their informed consent.

Measurement of bone area, BMD, BMC, lean mass and fat mass of lower extremity by dual energy X-ray absorptiometry

Bone area, BMD, BMC, fat mass, and lean mass of lower extremity were measured by dual energy X-ray absorptiometry (DXA) using a QDR-2000 densitometer (Hologic Inc., Waltham, MA. USA) in the array beam scanning mode (Enhanced Array Whole Body, version 5.60A). Regional bone area (cm^2) and BMD (g/cm^2) was measured in the head, upper extremities, lower extremities, ribs, thoracic spine, lumbar spine and pelvis. The lean mass (g), fat mass (g) and %Fat (%) of the head, upper extremities, lower extremities and trunk was measured with a tissue bar (11, 12). In our preliminary study, there was no significant difference of bone area, BMD, BMC, lean mass, fat mass and %Fat between dominant and non-dominant legs.

Figure shows the screen display of total bone mineral *in vivo*. Lines superimposed upon the skeleton demarcate major anatomical areas, head, upper extremities, ribs, thoracic spine, lumbar spine, pelvis and lower extremities. The horizontal line above the shoulders should be just below the chin. The vertical lines at the shoulders should be between the head of the humerus and scapula at the glenoid fossa. The vertical lines on either side of the spine should be moved close to the spine. The small horizontal line should be approximately at the level of L1-T12. The horizontal line above the pelvis should be just above the crest of the ilium. This line can be extended out at the sides to include soft tissue in the chest and waist. The angled lines below the pelvis should bisect both femoral necks. The vertical line between the lower extremities should be adjusted to be between the feet. The vertical lines lateral to the lower extremities should be adjusted to include as much of the soft tissue as possible in the thighs.

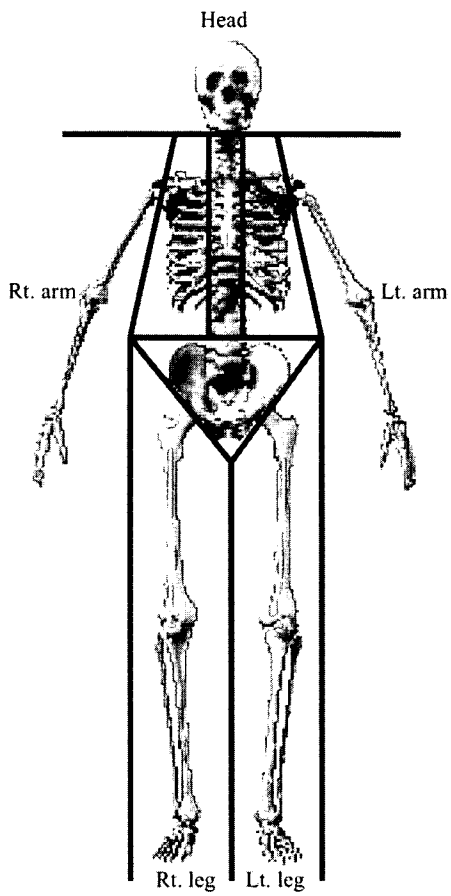

Figure Screen display of total bone mineral *in vivo*. Lines superimposed upon the skeleton demarcate major anatomical areas, head, upper extremities, ribs, thoracic spine, lumbar spine, pelvis and lower extremities.

Muscle strength

The isometric muscle strength of quadriceps and hamstrings muscles was measured with the knee

Table 1. Characteristics of men and women with unilateral ACL injury

	Age (y)	Body height (cm)	Body weight (kg)	BMI (kg/m^2)	Time from injury to admission (month)
Men (n=21)	21.3±6.2	172.6±4.1	66.5±5.9	22.4±2.3	11.6±14.3
Women (n=12)	26.3±8.2	161.3±4.7	59.1±8.0	22.7±3.0	16.7±15.0

BMI, body mass index

joint flexed in 45 degrees. The isokinetic muscle strength was assessed as a peak torque (Nm). The peak torque of the quadriceps and hamstrings was determined at a low-speed of 60 (degrees per second) and a high-speed of 180 (degrees per second) by means of an isokinetic machine using Cybex II. The injured/intact ratio of peak torque was compared between hamstring and quadriceps muscles at low-speed and high-speed to evaluate muscular contractility of the injured lower extremity.

Circumference of the thigh and circumference of the lower leg

The circumference of the thigh (COT) was measured at a point 10 cm proximal to the patellar superior pole, and the circumference of the lower leg (COLL) at the point of maximal diameter of the lower leg.

Statistics

Results were expressed as the mean±standard deviation. Student's paired t-test was used for differences between injured and intact legs of all patients. Spearman's rank correlation coefficients were calculated to correlate the time from injury to admission and injured lower extremity / intact lower extremity ratio of BMD, BMC, lean mass, fat mass, %fat, COT, COLL, muscle. A p value of less than 0.05 was considered to be statistically significant.

RESULTS

Bone area, BMD, BMC, lean mass, fat mass, %fat, COT and COLL (Table 2).

Significant effect of unilateral ACL injury on BMC, lean mass, fat mass, %fat, COT and COLL of the injured lower extremity was detected in this study.

BMC, lean mass, COT and COLL of the injured lower extremity were significantly smaller than those of the intact lower extremity ($p=0.0002$, $p<0.0001$, $p<0.0001$, $p=0.0131$). In contrast, fat mass and %Fat of the injured lower extremity were significantly greater than those of the intact lower extremity ($p=0.0301$, $p<0.0001$).

Muscle strength of hamstring and quadriceps muscles (Table 3).

The isometric muscle strength of hamstrings and quadriceps muscles of the injured lower extremity were significantly smaller than those of the intact lower extremity ($p<0.0001$, $p=0.0003$).

The isokinetic muscle strength, as expressed by peak torque (Nm), of the hamstring muscle of the injured lower extremity were significantly smaller than those of the intact lower extremity at low-speed and high speed ($p=0.0005$, $p=0.0006$). The isokinetic muscle strength of the quadriceps muscle of the injured lower extremity were significantly smaller than those of the intact lower extremity at low-speed and high speed ($p=0.0003$, $p=0.0037$).

Table 2. Bone area, BMD, BMC, lean mass, fat mass, COT and COLL of injured and intact lower extremities of all patients.

	Bone area (cm^2)	BMD (g/cm^2)	BMC (g)	Lean mass (g)	Fat mass (g)
Injured lower extremity	388.3±87.3	1.22±0.22	475.2±103.1	7,421.4±1,444.6	2,931.6±1,186.8
Intact lower extremity	405.1±94.9	1.23±0.18	493.0±105.2	7,821.3±1,507.1	2,861.0±1,148.3
p value	0.1995	0.6806	0.0002	<0.0001	0.0301

	%Fat (%)	COT (cm)	COLL (cm)
Injured lower extremity	27.0±10.5	43.4±3.1	35.5±2.7
Intact lower extremity	25.3±9.9	44.7±3.5	36.0±2.9
p value	<0.0001	<0.0001	0.0131

Values given as the mean ± standard deviation.
BMD, bone mineral density ; BMC, bone mineral content ; COT, circumference of the thigh ; COLL, circumference of the lower leg

Table 3. Muscle strength of quadriceps and hamstring muscles of injured and intact lower extremities of all patients.

(A) Hamstring muscle strength

	Isometric	Low-speed (60 degrees/second)	High-speed (180 degrees/second)
Injured lower extremity (Nm)	81.6±34.4	64.9±25.6	62.5±22.9
Intact lower extremity (Nm)	98.9±35.9	83.0±28.1	76.0±24.9
p value	<0.0001	0.0005	0.0006

Values given as the mean±standard deviation.

(B) Quadriceps muscle strength

	Isometric	Low-speed (60 degrees / second)	High-speed (180 degrees / second)
Injured lower extremity (Nm)	155.7±74.8	107.4±52.1	99.8±47.2
Intact lower extremity (Nm)	197.4±73.2	156.4±57.5	127.1±42.0
p value	0.0003	0.0003	0.0037

Values given as the mean±standard deviation.

Table 4. Relationship between the time from injury to admission and injured lower extremity / intact lower extremity ratio of Bone area, BMD, BMC, fat mass, lean mass, muscle strength and COT, COLL of all patients.

	ρ	p value
Inj/int Bone area of the lower extremity	0.208	0.247
Inj/int BMD of the lower extremity	-0.232	0.197
Inj/int BMC of the lower extremity	-0.249	0.166
Inj/int Fat of the lower extremity	-0.388	0.031
Inj/int Lean of the lower extremity	0.111	0.538
Inj/int Hamstring muscle strength		
isometric	-0.530	0.056
low-speed (60 degrees/second)	-0.079	0.775
high-speed (180 degrees/second)	-0.263	0.344
Inj/int Quadriceps muscle strength		
isometric	0.029	0.918
low-speed (60 degrees/second)	-0.206	0.468
high-speed (180 degrees/second)	-0.075	0.788
Inj/int COT	0.055	0.812
Inj/int COLL	0.199	0.386

BMD, bone mineral density ; BMC, bone mineral content ; COT, circumference of the thigh ; COLL, circumference of the lower leg

Relationship between the time from injury to admission and injured lower extremity / intact lower extremity ratio of BMD, BMC, lean mass, fat mass, %fat, COT, COLL, muscle strength (Table 4).

The time from injury to admission to our hospital was 3 to 60 months, with an average of 14.5±15.0 months. There was a significant negative correlation between the time from injury to admission and injured / intact ratio of fat mass of lower extremities (p=0.031).

DISCUSSION

Chronic unilateral ACL insufficiency reduced BMC of the injured lower extremity, whereas BMD did not change between the injured lower extremity and intact lower extremity. Kannus, *et al.* (7) showed that a cruciate ligament injury resulted in decreased BMD of the distal femur, patella and proximal tibia in the injured knee. In this study, we measured BMC, BMD and the soft tissue composition of the lower extremity as shown in Figure. In the future study,

we should measure the BMDs of the proximal femur, distal femur, patella, proximal tibia and calcaneus of both lower extremities to study the effects of an unilateral ACL injury on BMD.

The most important determinant to maintain the BMD of weight bearing bones is the mechanical load applied to the bones. Osteocytes embedded in the bone matrix play an important role in responding to mechanical stress on bone and metabolism changes in bone (13-15). Osteocytes have long processes to conduct mechanical load to other osteocytes, osteoblasts or osteoclasts (16). The gap junction of the long processes enables osteocytes to transmit mechanical stress to facilitate bone formation by osteoblasts while inhibiting bone resorption by osteoclasts in axial bones and appendicular bones. Except for the acute period after ACL injury, these patients could walk with full weight bearing, which may prevent reduction of the BMD of the injured leg in spite of the decrease in BMC.

ACL injury was associated with a reduction of the muscle strength of the injured lower extremity in this study, which is ascribable to disuse muscle atrophy resulting from a decrease in the synthesis of contractile proteins and acceleration of degradation of muscle proteins. In addition, the degree of loss of quadriceps muscle peak torque at low-speed was greater than that of the hamstring muscle, indicating that the quadriceps muscle on the ACL-injured side is more susceptible to lose muscle strength and muscle mass than the hamstrings muscles. The quadriceps muscle is one of the antigravity muscles. Therefore, quadriceps muscles may be predominantly affected by disuse and immobilization than hamstrings muscles. Previous studies have shown that chronic ACL injury affects predominantly quadriceps muscles compared with hamstrings muscles (2, 5, 17, 18), and that it particularly affects the vastus medialis muscles within quadriceps muscles (18). Weakness and atrophy of the quadriceps muscles on the injured side, as shown in the present study, may have been due to selective muscle atrophy of the vastus medialis muscle.

There was a significant negative correlation between injured / intact ratio of fat mass of lower extremities and the time from injury to admission, as shown in Table 3 ($p=0.031$). Based on this fact, fat mass of the injured lower extremity changed with time more markedly than the lean mass of the injured lower extremity.

The present study was just a cross sectional study of patients with unilateral ACL injury before ACL reconstruction. Therefore, a longitudinal study should be carried out to clarify the effects of surgery on the musculoskeletal system of the lower extremity.

REFERENCES

1. McDaniel WJ, Dameron TB : The untreated anterior cruciate ligament injury. Clin Orthop 173 : 158-163, 1983
2. Corrigan JP, Cashman WF, Brady MP : Proprioception in the cruciate deficient knee. J Bone Joint Surg 74B(2) : 247-250, 1992
3. Murray SM, Warren RF, Otis JC, Kroll M, Wickiewicz TL : Torque-velocity relationships of the knee extensor and flexor muscles in individuals sustaining injuries of the anterior cruciate ligament. Am J Sports Med 12 : 436-440, 1984
4. Tegner Y, Lysholm J, Gillquist J, Oberg B : Two-year follow-up of conservative treatment of knee ligament injuries. Acta Orthop Scand 55 : 176-180, 1984
5. Baugher WH, Warren RF, Marshall JL, Joseph A : Quadriceps atrophy in the anterior cruciate insufficient knee. Am J Sports Med 12 : 192-195, 1984
6. Sievanen H, Kannus P, Heinonen A, Oja P, Vuori I : Bone mineral density and muscle strength of lower extremities after long-term strength training, subsequent knee ligament injury and rehabilitation : A unique 2-year follow-up of a 26-year-old female student. Bone 15 (1) : 85-90, 1984
7. Kannus P, Sievanen H, Jarvinen M, Heinonen A, Oja P, Vuori I : A cruciate ligament injury produces considerable, permanent osteoporosis in the affected knee. J Bone Miner Res 7 (12) : 1429-1434, 1992
8. Curl WW, Markey KL, Mitchell WA : Agility training following anterior cruciate ligament reconstruction. Clin Orthop 172 : 133-136, 1983
9. Steadman JR : Rehabilitation of acute injuries of the anterior cruciate ligament. Clin Orthop 172 : 129-132, 1983
10. Clancy WG, Nelson DA, Reider B : Anterior cruciate ligament reconstruction using one third of the patellar ligament, augmented by extra-articular tendon transfer. J Bone Joint Surg 62A : 352-359, 1982
11. Takata S, Ikata T, Yonezu H : Characteristics

of regional bone mineral density and soft tissue mass in patients with atraumatic vertebral fractures. J Bone Miner Metab 18(5) : 287-290, 2000
12. Takata S, Ikata T, Yonezu H, Inoue A : Effects of lower leg lengthening on bone mineral density and soft tissue composition of legs in a patient with achondroplasia. J Bone Miner Metab 18(6) : 339-341, 2000
13. Cowin SC, Moss SL, Moss ML : Candidate for the mechanosensor system in bone. J Biomech Eng 113(2) : 191-197, 1982
14. Doty SB : Morphological evidence of gap junctions between bone cells. Calcif Tissue Int 33 (5) : 509-512, 1981
15. Lanyon LE : Osteocyte, strain detection, bone modeling and bone remodeling. Calcif Tissue Int 53 : S102-S107, 1993
16. Palumbo C, Palazzini S, Marotti G : Morphological study of intercellular junctions during osteocytes differentiation. Bone 11(6) : 401-406, 1990
17. Nakamura T, Kurosawa H, Kawahara H, Watarai K, Miyashita H : Muscle fiber atrophy in the quadriceps in knee-joint disorders. Histochemical studies on 112 cases. Arch Orthop Trauma Surg 105(3) : 163-169, 1986
18. Gerber C, Hoppeler H, Claassen H, Robotti G, Zehnder R, Jakob RP : The lower-extremity musculature in chronic symptomatic instability of the anterior cruciate ligament. J Bone Joint Surg 67-A : 1034-1043, 1985

BRAIN RESEARCH 1137 (2007) 20–28

available at www.sciencedirect.com

ScienceDirect

www.elsevier.com/locate/brainres

BRAIN RESEARCH

Research Report

Transient suppression of the vesicular acetylcholine transporter in urinary bladder pathways following spinal cord injury

Yuki Takahara[a,b], Mitsuyo Maeda[a], Tatsuya Nakatani[b], Hiroshi Kiyama[a,*]

[a]Department of Anatomy and Neurobiology, Osaka City University Graduate School of Medicine, 1-4-3 Asahimachi, Abenoku, Osaka 545-8585, Japan

[b]Department of Urology, Osaka City University Graduate School of Medicine, 1-4-3 Asahimachi, Abenoku, Osaka 545-8585, Japan

ARTICLE INFO

Article history:
Accepted 14 December 2006
Available online 21 December 2006

Keywords:
VAChT
Pelvic ganglion
Bladder
Regeneration
Micturition

ABSTRACT

The aim of this study was to examine the expression profile of the vesicular acetylcholine transporter (VAChT), which is a cholinergic pre-synaptic marker, in the lower neural tract following spinal cord injury (SCI) and its effect on coordination of micturition. In adult female Sprague–Dawley rats, SCI was induced by complete transection of the spinal cord at T9. At various time points, 3, 7, 14 and 28 days, after SCI, cystometry was performed on conscious rats. Bladder areflexia was observed during the first week. Twenty-eight days after SCI the rats showed reflex contractions and voiding. The expression of VAChT was examined with immunohistochemistry. The number of VAChT-positive nerve terminals, which were surrounding neuronal soma, was transiently decreased in pelvic ganglion and spinal cord (L1, L2, L6 and S1). In particular VAChT terminals surrounding motor neurons in the ventral horn and autonomic pre-ganglion cells were dramatically decreased from 3 to 14 days after SCI. Similarly, and the number of VAChT-positive fibers in the bladder wall was also decreased. The intensity of VAChT terminals recovered in all above regions in conjunction with recovery of bladder function. These observations indicate that the transient decrease of the VAChT-positive nerve might cause a failure of cholinergic neuronal transmission along the urinary bladder tract after SCI. As the cholinergic system was recovered at least in rat, the functional recovery of neurogenic bladder syndrome in SCI patients may become possible by further understanding the mechanism underlying the recovery of cholinergic system in rat.

1. Introduction

Spinal cord injury (SCI) above the lumbosacral level causes a phase of spinal shock and impairs voluntary micturition (de Groat, 1995; de Groat et al., 1990; Kruse et al., 1993). Concomitantly, it evokes inhibition of sphincter activity resulting in a hyperreflexia of the bladder and the external sphincter (detrusor–sphincter–dyssynergia) (Kruse et al., 1994; Seki et al., 2002; Yoshiyama et al., 1999). Also SCI induces functional bladder outlet obstruction, and increasing

* *Corresponding author.* Fax: +81 666 45 3702.
E-mail address: kiyama@med.osaka-cu.ac.jp (H. Kiyama).

Abbreviations: BSA, bovine serum albumin; ChAT, choline acetyl transferase; FDI, fiber density index; IR, immunoreactivity; PBS, phosphate buffer saline; Per, peripherin; SCI, spinal cord injury; VAChT, vesicular acetylcholine transporter

0006-8993/$ – see front matter © 2006 Elsevier B.V. All rights reserved.
doi:10.1016/j.brainres.2006.12.042

micturition pressure and detrusor muscle hypertrophy (Keast, 1999; Kruse et al., 1995; Yoshiyama et al., 1999). And it is known that rat and human exhibit similar micturition dysfunction after SCI (Kruse et al., 1993). However, in rat the bladder reflex activity slowly recovers within a few weeks following SCI and initiates voluntary micturition in chronic paraplegic animals (Chancellor et al., 1994). Thus, understanding the molecular mechanisms implicated in the hypofunction and subsequent amelioration after SCI would provide a basis for enhancing reorganization of lower urinary tract function after SCI in humans.

Micturition consists of two main functions, storage and voiding, and the voluntary control of voiding is regulated by a complex mechanism in the spinal and supraspinal neural pathways (Hoang et al., 2006). In rats, voiding is normally mediated by contraction of the detrusor accompanied by coordinated activation of the external sphincter (de Groat, 1995; de Groat et al., 1990; Pikov and Wrathall, 2001). Motor neurons activating the external sphincter are located in the dorsolateral nucleus of the L6–S1 ventral horn (Pikov and Wrathall, 2001; Schroder, 1980), and those activating the bladder are part of sacral parasympathetic nuclei (Nadelhaft and Booth, 1984; Pikov and Wrathall, 2001), receive direct or indirect supraspinal projections mainly from Barrington's nucleus (Marson, 1997; Nadelhaft and Vera, 1996; Vizzard et al., 1995) in the brain stem. Efferent pathways from the thoracolumbar (T12–L2) and lumbosacral (L5–S1) levels of the spinal cord project to the lower urinary tract via nerves as follows: (1) the hypogastric nerve, which carries sympathetic pre-ganglionic inputs from lumbar cord, or (2) pelvic nerve, which carries parasympathetic inputs from sacral cord; the and (3) pudendal nerve, whose motor neurons originate in the ventral horn of segments L6–S1 (Callsen-Cencic and Mense, 1999; Marson and Gravitt, 2004; McKenna and Nadelhaft, 1986). Accordingly, orchestration of those systems could be crucial for micturition.

In order to evaluate activities of those efferent pathways morphologically, identification of cholinergic inputs would be useful because those systems use acetylcholine as a major neurotransmitter (Schafer et al., 1994). To examine the alteration of cholinergic synaptic inputs, we focused on the vesicular acetylcholine transporter (VAChT) as a marker for the cholinergic pre-synapse area. VAChT is a vesicle membrane protein and is responsible for the uptake of acetylcholine into synaptic vesicles (Erickson et al., 1996; Ferguson et al., 2003; Maeda et al., 2004). Both expression of VAChT mRNA and protein was demonstrated in a variety of cholinergic neurons, including peripheral motor and autonomic nerves (Arvidsson et al., 1997; Schafer et al., 1998). The most important feature of VAChT is its fairly restricted localization on cholinergic synaptic vesicles, and therefore every cholinergic terminal including autonomic and motor termini can be clearly visualized by immunohistochemistry using anti-VAChT antibody (Maeda et al., 2004; Schafer et al., 1998; Weihe et al., 1996). Furthermore, it was demonstrated that after cranial motor nerve injury, the protein levels of VAChT in endplate transiently disappeared, and along with the nerve regeneration the VAChT immunoreactivity recovered in the regenerated pre-synaptic terminal (Maeda et al., 2004). This suggested that the recovery of VAChT immunoreactivity in pre-synaptic terminals corresponded to the functional recovery. Therefore, here we have examined the alterations of VAChT expression in synaptic terminals of the urinary bladder pathway including spinal cord, pelvic ganglion and bladder after SCI.

2. Results

2.1. *Cystometry*

During the awake-cystometry, an infusion of saline into the bladder induced rhythmic bladder reflex contractions in normal rats, and bladder pressure during the infusion rapidly increased without detectable contractile activity until the initiation of reflex voiding. The amplitude (26.1±2.8 cm H_2O), duration (22.4±3.0 s) of bladder contractions and voided volume (0.4±0.1 ml) were similar to the measurements among normal rats (Fig. 1A). Voiding was totally abolished during the first week after SCI. At 3 days after SCI, bladder contractions were not observed at all (Fig. 1B). Then irregular bladder contractions started to occur at 7 days, though this voiding was not efficient enough to empty the bladder (Fig. 1C). From this period, the automatic micturition gradually returned. The activity of distended and hypertrophied bladder was clearly increased at 14 days post-operation (Fig. 1D). At 28 days, the high amplitude (40.7±3.4 mm H_2O) and long duration (35.3±6.0 s) following small amplitude (5.1±2.4 mm H_2O) contractions appeared and the voided volume (4.9±1.9 ml) increased (Fig. 1E). The bladders of SCI rats were notably distended resulting in increased voided volume, but the residual urine was still present 28 days following SCI.

2.2. *Immunohistochemistry*

2.2.1. *VAChT-IR in bladder*

The bladders of SCI rats were distended and the bladder walls markedly thickened compared with that of normal rats at the time of bladder removal. In normal rats, VAChT-IR nerve fibers with varicosities were present along the detrusor bundle (Fig. 2A), and some minor populations of positive fibers were also observed in the lamina propria. To examine whether VAChT-IR structures corresponded to nerve, we have attempted the simultaneous labeling with the antibody against the pan-PNS nerve marker, peripherin (Per). All VAChT-positive fibers were simultaneously stained with peripherin immunoreactivity (Per-IR), although some Per-IR-positive fibers were negative to VAChT-IR suggesting that VAChT-IR-negative fibers would be sensory or sympathetic nerves. Initially we have examined both base and body parts of the bladder, and the fiber intensity was significantly higher in base part than in body. However, the alterations of the density of VAChT-IR fibers in the both regions after SCI demonstrated similar tendencies. Therefore, we presented the cases observed in base part of the bladder in this paper. In SCI animals VAChT-IR nerve fibers in the bladder walls were significantly decreased at 3 days after SCI (Fig. 2B), and further decreased at 7 days after SCI (the fiber density index: FDI 0.6±0.6, Figs. 2C and 3) compared with normal rats (FDI: 7.8±2.8, $p<0.001$). All the VAChT-IR fibers remained were

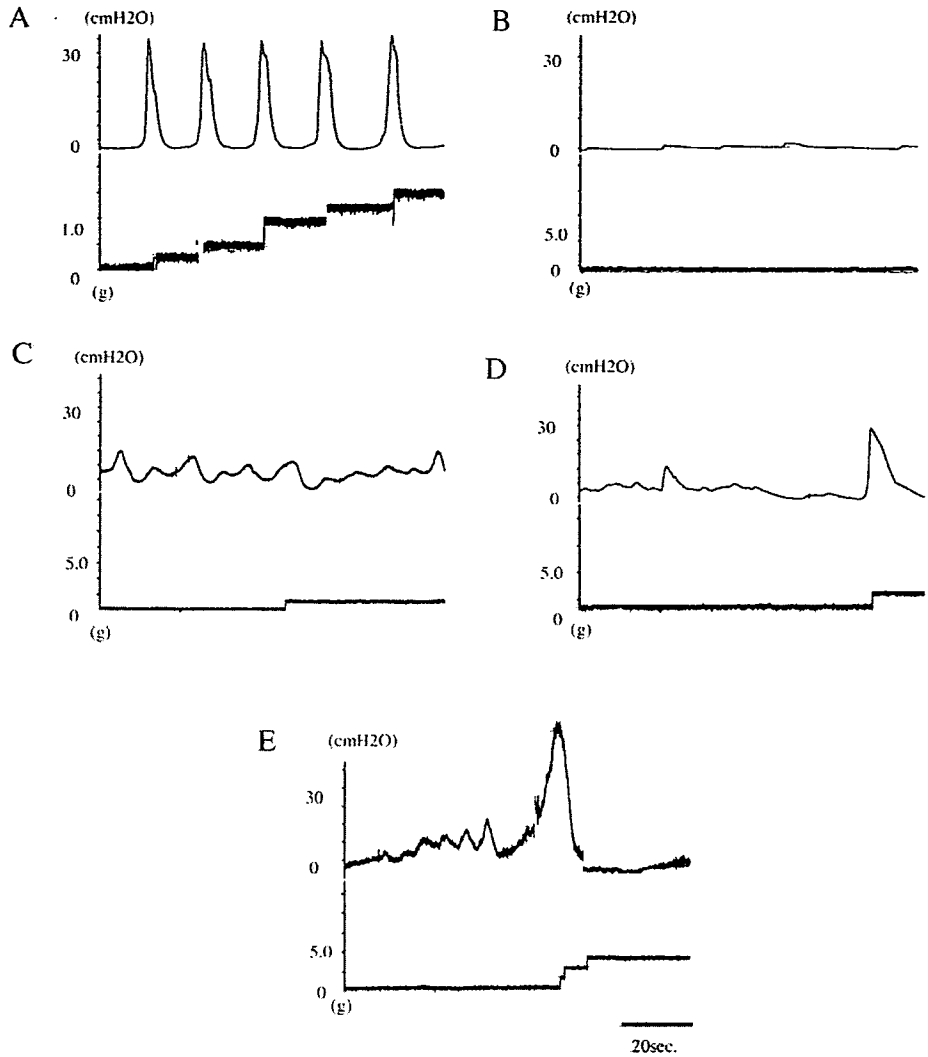

Fig. 1 – Cystometry in control and spinal cord injury (SCI) rats. The upper section showed bladder pressure, and the lower voided volume. (A) Control, (B) at 3 days after SCI, (C) at 7 days, (D) at 14 days and (E) at 28 days.

also positive to the Per-IR. Although the intensity of Per-IR fibers was decreased compared with those in normal, significant Per-IR-positive and VAChT-IR-negative fibers remained (Fig. 2C). The VAChT-IR nerve fibers increased gradually along the detrusor bundle at 14 days following SCI (FDI: 1.8±0.7; Fig. 2D), but the fiber intensity did not return to the normal level at 28 days post-injury (FDI: 4.0±1.1; Fig. 2E).

2.2.2. *VAChT-IR in pelvic ganglion*

In the pelvic ganglion of normal rats, most neuron cell bodies were attached or surrounded by very intense VAChT-IR varicose nerve terminals, which showed loose basket-like formation (95.3±6.3%; Fig. 4A). VAChT-IR was not observed within the cell bodies of neurons, although most of cells were supposed to be cholinergic neurons, suggesting the localization of VAChT is restricted to pre-synaptic nerve terminals and not in soma. During the first week after SCI, the number of neurons with VAChT-IR terminals was significantly decreased. Although the decrease of the neurons with VAChT-IR was not significant at 3 days after SCI (64.2±29.4%; Fig. 4B), the decrease at 7 days after SCI was significant compared to control rats (31.3±17.2%, $p<0.05$; Fig. 4C). At 14 days after SCI the number of neurons with VAChT-IR terminals was slightly increased (43.1±12.4%; Fig. 4D), but the number of VAChT-IR terminals was still low. In addition, the thickness of VAChT-IR varicose nerve terminals seen in animals 14 and 28 days after SCI were smaller than those in controls. An increase of VAChT-IR terminals was observed at 28 days after SCI (52.3±8.8%; Fig. 4E); however, the number of neurons with VAChT-IR terminals did not return to the normal level.

2.2.3. *VAChT-IR in spinal cord*

Spinal segments L1, L2, L6 and S1 were examined for VAChT-IR. In normal rats, very intense VAChT-IR was observed in nerve terminals, which were surrounding cell bodies of motor neurons in the ventral horn (Fig. 5A), sympathetic pre-ganglionic cells in intermediolateral nucleus (L1–L2) and sacral parasympathetic neurons, which were present at the outer edge of lamina VII in L6–S1 (Fig. 5B). Although those neurons

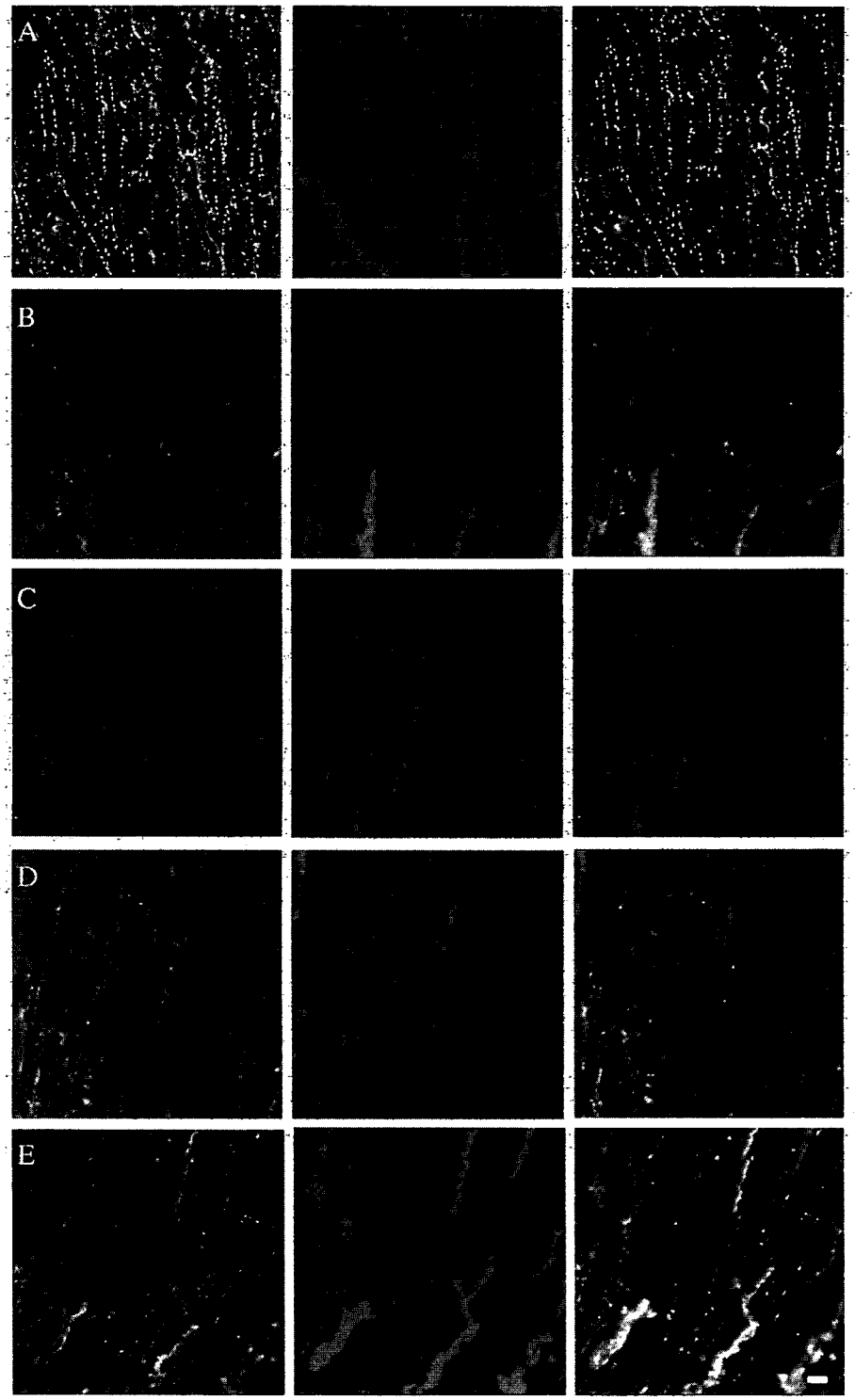

Fig. 2 – Double immunolabeling for VAChT (green) and peripherin (red) in bladder wall. (A) control, (B) at 3 days after SCI, (C) at 7 days, (D) at 14 days and (E) at 28 days. Scale bar=40 μm. (For interpretation of the references to colour in this figure legend, the reader is referred to the web version of this article.)

are obviously cholinergic, the immunoreactivity was faint and not discrete, suggesting that most of VAChT in those cholinergic neurons was restricted to nerve terminals. At 3 days after SCI, VAChT-IR in the nerve terminals around the motor neurons in the ventral horn was remarkably decreased (Fig. 5C). In addition the VAChT-IR terminals in the intermediolateral nucleus and sacral parasympathetic nucleus were dramatically decreased (Fig. 5D). At 7 days following SCI, the density of VAChT-IR terminals was almost the same as at day 3 (Figs. 5E, F). The density of VAChT-IR terminals in

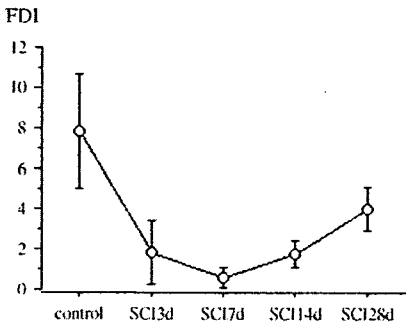

Fig. 3 – The fiber density index (FDI) in control and SCI rats. FDI is presented as mean±SD; *$P<0.05$ (Student *t*-test).

every region was increased 14 days after SCI (Figs. 5G, H), and thereafter the intensity of VAChT-IR terminals were increased by 28 days post-injury. At 28 days post-injury, the density of VAChT-IR terminals in all regions had returned to control levels (Figs. 5I, J).

3. Discussion

The present study morphologically demonstrated that cholinergic pre-synaptic inputs, which were visualized by VAChT staining, were suppressed at various levels along the neural tract after SCI. VAChT is predominantly located on the cholinergic synaptic vesicle membrane and functions to accumulate acetylcholine inside synaptic storage vesicles. This makes it a useful and reliable tool not only for visualizing cholinergic nerve terminals specifically, but also for detecting functional cholinergic axon terminals morphologically (Erickson et al., 1996; Ferguson et al., 2003; Maeda et al., 2004; Weihe et al., 1996). In fact previous studies demonstrated a correlation between the appearance of VAChT and the functional nerve regeneration using the peripheral nerve injury model (Maeda et al., 2004; Matsuura et al., 1997). The dysfunction of cholinergic neurotransmission along the tract due to the decrease of VAChT may be a major reason for the neurogenic bladder syndrome.

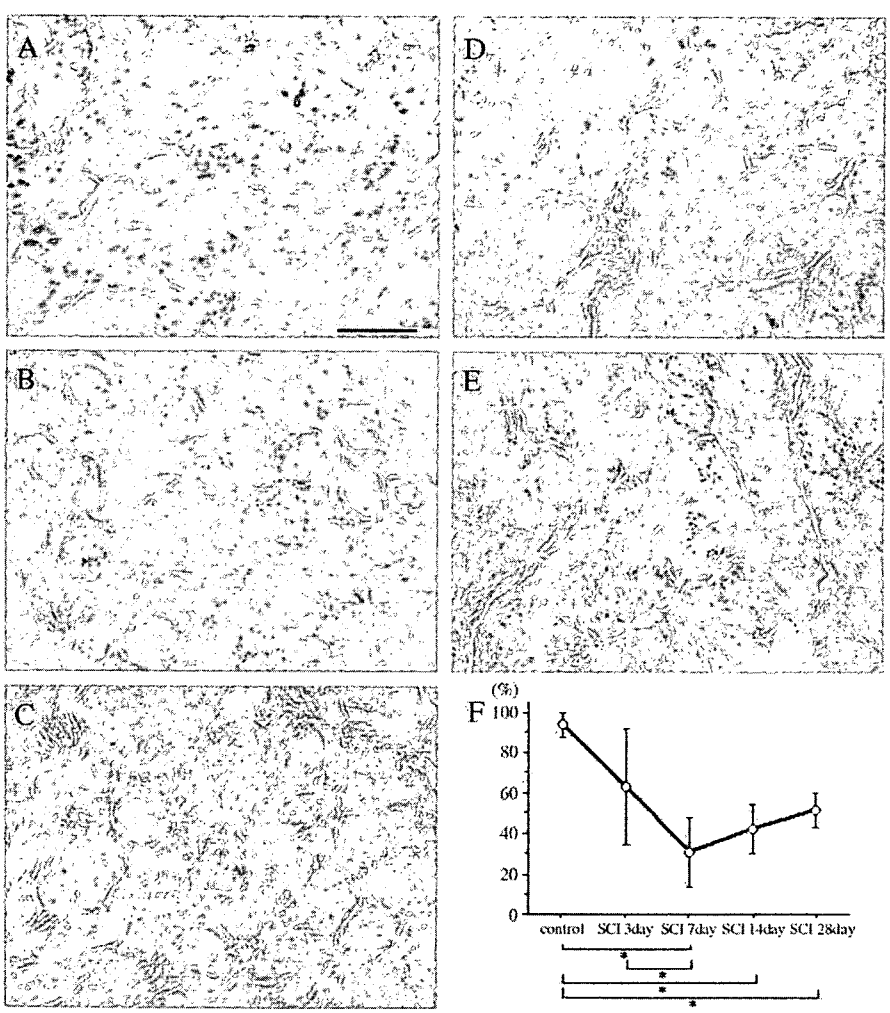

Fig. 4 – VAChT-IR in pelvic ganglion immunostaining. (A) control, (B) at 3 days after SCI, (C) at 7 days, (D) at 14 days and (E) at 28 days. (F) The proportion of the neuronal cells with VAChT-IR nerve terminals in all neurons of pelvic ganglion were counted in control and SCI rats and presented as mean±SD; *$P<0.05$ (Student *t*-test). Scale bar=40 μm.

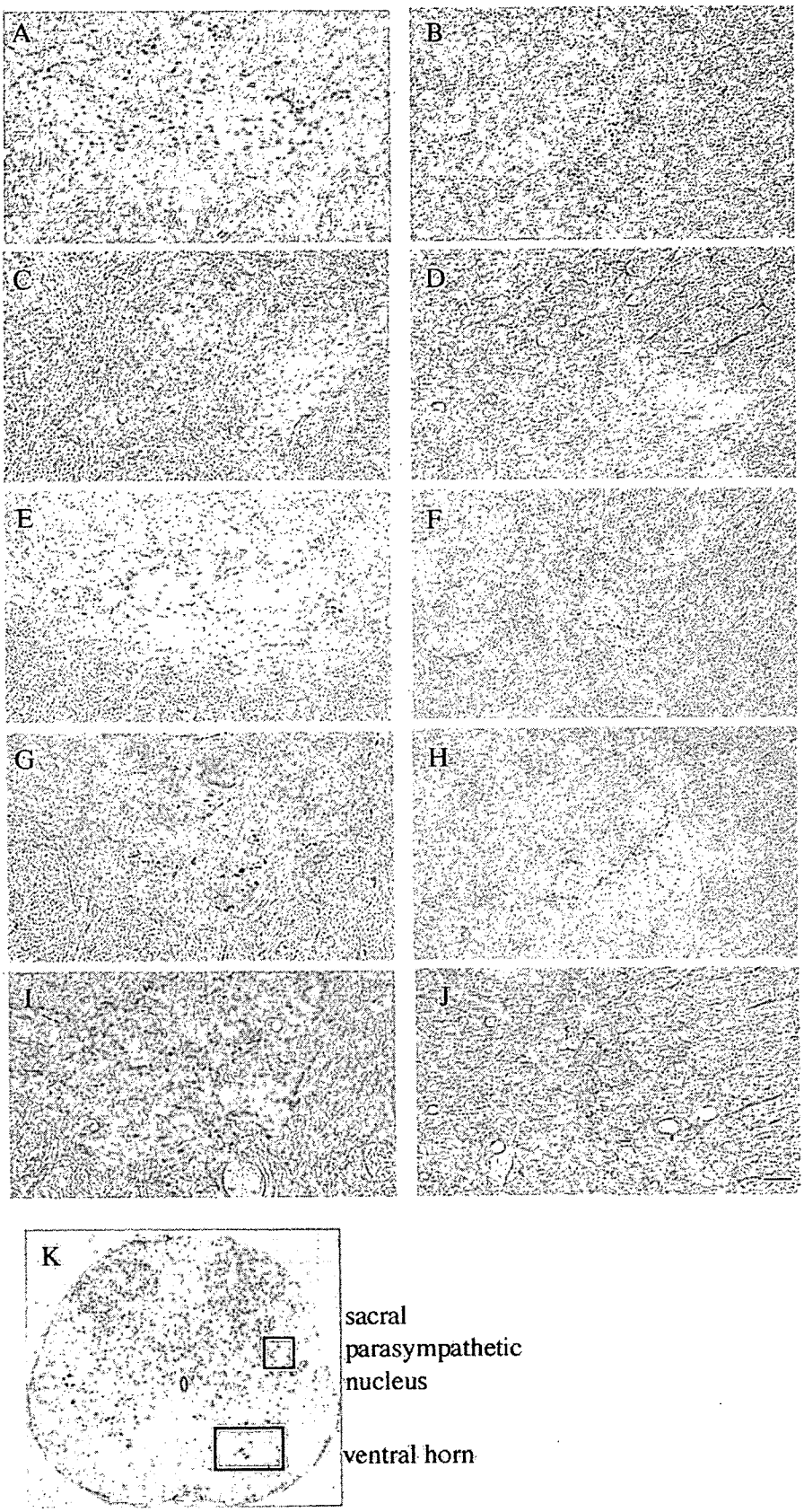

Fig. 5 – VAChT-IR in S1 level of spinal cord immunostaining. (A, B) In control rats, (C, D) 3 days, (E, F) 7 days, (G, H) 14 days and (I, J) 28 days after SCI. (A, C, E, G, I) ventral horn and (B, D, F, H, J) the area of sacral parasympathetic nucleus. (K) The representative Nissl-stained photograph of S1 level of spinal cord demonstrating the regions we examined in panels A–J. Scale bar=20 μm.

In this study, we used a model of complete transection of rat spinal cord to investigate how an absolute disconnection between the brain and lower spinal cord affected the reorganization of the spinal reflex mechanism. The complete transection of the spinal cord produced the bladder areflexia in which no voiding occurred during the first week. However, the rats examined 28 days after SCI showed reflex contractions and voiding, although this reflex contraction was induced by intravesical instillation of a large volume of saline. The reflex contractions accompanied with larger amplitude, longer duration and irregular intervals compared with control rats. The appearance of VAChT-IR nerve terminals in the bladder was in parallel with the recovery of bladder function, although the recovered VAChT-IR terminals were slightly less abundant than in controls. This finding supports a strong correlation between the transient bladder function deficit and the decrease of VAChT-IR in the bladder following SCI.

In terms of the transient decrease of VAChT-IR terminals seen in the bladder, pelvic ganglion and spinal cord following SCI, the decrease in the spinal cord appear to precede the pelvic ganglion and bladder. This might be a direct consequence of the complete transection of supraspinal projections. The loss of innervations including cholinergic as well as others on the autonomic pre-ganglion neurons and motor neurons might give rise to dysfunction in those spinal neurons. These dysfunctions might secondarily cause the decrease of VAChT-positive terminals in the pelvic ganglion and bladder. The decreased VAChT-IR was recovered to some extent at 28 days after SCI, suggesting that re-innervation and/or re-expression of VAChT might occur, although the origin of the terminal was not clear. Two possibilities would be conceivable as for the reasons why those VAChT-IR terminals had disappeared after SCI. One is the disappearance of VAChT protein in the nerve terminal, and another could be the disappearance of the pre-synaptic structure itself. Since the gene encoding VAChT is located within the gene encoding choline acetyl transferase (ChAT), the transcription of both ChAT and VAChT genes are regulated in a similar manner (Erickson et al., 1996; Matsuura et al., 1997; Usdin et al., 1995). This would be quite expected because the synthesis of acetylcholine and its packaging have to be processed simultaneously for the functional cholinergic synaptic transmission. Several previous reports demonstrated suppression of ChAT after various types of neural injury (Jacobsson et al., 1998; Piehl et al., 1993; Wooten et al., 1978). Therefore, the suppression of VAChT is also likely after SCI. In this situation, the pre-synaptic terminal structure may be maintained. Alternatively, it is also possible that some pre-synaptic structures may be retracted as a secondary effect of SCI and the retracted nerve terminals may start sprouting a few weeks after SCI, leading to recovery of the bladder function. The latter possibility is more likely at least in the bladder because the decrease of Per-IR, which was a pan-PNS marker, was evident in the bladder after SCI. As shown in earlier studies that sprouting occurs rapidly after removal of pre-ganglionic inputs in pelvic ganglion, and their source may be the ganglion cells in pelvic ganglion (Keast, 2004; Kepper and Keast, 1998). The sprouting among the peripheral nerve system may be an essential mechanism for the recovery of bladder function (Krenz and Weaver, 1998). Although all neurons, including spinal neurons and pelvic ganglion, did not suffer from direct injuries in SCI, the indirect insult such as functional failure of pre-synaptic inputs might promote such retraction and sprouting. In any event it is noteworthy that the cholinergic terminal recovery was observed at each level of the pathway.

In conclusion, the recovery of cholinergic nerve terminals at each level of the pathway after SCI is pivotal for the recovery of bladder function. Also, the reappearance of those terminals as quickly as 28 days after SCI suggests that the neuronal circuits downstream from lumbosacral spinal neurons, that regulate micturition, are likely to be intact or rather have high plasticity. Therefore, at least in the rostral SCI patients the activation of cholinergic system including the expressions of both VAChT and ChAT as well as the induction of the sprouting of the cholinergic nerve may lead to a recover of the bladder function.

4. Experimental procedures

4.1. *Animals and surgical procedure*

Female Sprague–Dawley rats (weight 230–300 g, SLC, Japan) were used in all the experiments ($n=50$). Twelve animals were used as normal controls with an intact spinal cord. The animals were anesthetized by intramuscular injection of ketamine (50 mg/kg) and xylazine (5 mg/kg). After exposure of the dorsal process of the ninth thoracic (T9) vertebra, laminectomy (T8–T9) was performed to expose the spinal cord, and the spinal cord was completely transected at the T9 spinal segment, with fine scissors. The muscles and skin above the laminectomy were closed.

To prevent over-distension of the bladder of operated animals, urine in the bladder was pressed out manually twice a day until automatic micturition developed. The level and completeness of spinal transection was histologically confirmed post-mortem after physiological experiments. The animals were examined within 3–28 days after spinal cord injury (SCI).

Experiments were carried out in accordance with the Guideline laid down by Osaka City University Medical School regarding the care and use of animals for experimental procedures.

4.2. *Cystometry*

After anesthesia with halothane (1.5%), the bladder was exposed via a midline abdominal incision. A polyethylene catheter (SP-45, ID 0.58 mm; Natsume Seisakusyo, Japan) was inserted through a small incision into the bladder dome and secured with a ligature. Then the next day, the other end of catheter was connected via tube to a TE-311 (Terumo Co., Ltd., Japan) pump for continuous infusion of physiological saline and also to an MLT0670 (AD Instruments, Inc., Australia) pressure transducer to record intravesical pressure monitoring with PowerLab system (AD Instruments, Inc.). Saline was infused into the bladder at room temperature (at a constant rate of 0.04 ml/min for control rats, 0.1 ml/min for SCI rats) to elicit repeated voiding responses. Saline voided from the urethral meatus was collected and measured to determine voided volume.

4.3. *Immunohistochemistry*

Under anesthesia with ether, transcardiac perfusion with 150 ml saline solution followed by 500 ml of 0.15% picric acid and 2% paraformaldehyde in 0.1 M phosphate-buffered saline (PBS) (pH 7.4) was performed. After perfusion, the bladder, pelvic ganglion and spinal cord were immediately removed, post-fixed in the same fixative and cryoprotected by immersion in 30% sucrose in PBS. The bladder sections were initially divided in two parts, the bladder base and body, and each part was examined. After preliminary experiment, the bladder base was mainly used.

Cryostat sections of bladder (16 μm thick), pelvic ganglion (10 μm thick) and spinal cord (25 μm thick) were incubated in 1% Triton X-100 in PBS. Nonspecific binding sites were blocked in 0.3% Triton X-100/1% bovine serum albumin (BSA) in PBS. Then the sections were incubated with goat polyclonal antibody against VAChT (1:500; Santa Cruz, CA) in 0.3 % Triton X-100/1% BSA in PBS overnight at 4 °C. On the next day, sections were incubated with rabbit biotinylated anti-goat IgG (1:500; Vector Laboratories, CA) and incubated in avidin–biotin horseradish peroxidase complex (Vector Laboratories Inc.) in PBS. Staining was visualized with 3, 3′ diaminobenzidine tetrahydrochloride (0.2 mg/ml; Vector Laboratories Inc.). For double labeling with peripherin, a marker for PNS nerve, the bladder sections were stained with a cocktail of VAChT antibody as described plus rabbit polyclonal antibody against peripherin (1:500; Chemicon International, Temecula, CA) in 0.3% Triton X-100/1% BSA in PBS overnight at 4 °C. Then the tissues were incubated with Alexa-Fluor 488 donkey anti-goat IgG (1:500; Invitrogen, Oregon). Following a stringent rinse, they were incubated with Alexa-Fluor 594 goat anti-rabbit IgG (1:500; Molecular Probes, Oregon) for 2 hours.

4.4. *Statistics*

In pelvic ganglion from normal and SCI rats, the neuronal cells with VAChT immunoreactivity (IR) in nerve terminals were counted in 5 sections from each animal. In bladder detrusor, VAChT-IR fibers that crossed the range of 100 μm vertically were counted in 3 sections from the bladder base part from each animal. They were averaged out and defined as fiber density index; FDI. Data were expressed as the mean±SD. Statistical comparisons were performed by Student's unpaired *t*-tests with a significance level of $p<0.05$.

Acknowledgments

We are grateful to C. Kadono and I. Jikihara for technical assistance and T. Kawai for secretarial assistance. This study was supported in part by grants from the Ministry of Health, Labor and Welfare of Japan and the MEXT.

REFERENCES

Arvidsson, U., Riedl, M., Elde, R., Meister, B., 1997. Vesicular acetylcholine transporter (VAChT) protein: a novel and unique marker for cholinergic neurons in the central and peripheral nervous systems. J. Comp. Neurol. 378, 454–467.

Callsen-Cencic, P., Mense, S., 1999. Increased spinal expression of c-Fos following stimulation of the lower urinary tract in chronic spinal cord-injured rats. Histochem. Cell Biol. 112, 63–72.

Chancellor, M.B., Rivas, D.A., Huang, B., Kelly, G., Salzman, S.K., 1994. Micturition patterns after spinal trauma as a measure of autonomic functional recovery. J. Urol. 151, 250–254.

de Groat, W.C., 1995. Mechanisms underlying the recovery of lower urinary tract function following spinal cord injury. Paraplegia 33, 493–505.

de Groat, W.C., Kawatani, M., Hisamitsu, T., Cheng, C.L., Ma, C.P., Thor, K., Steers, W., Roppolo, J.R., 1990. Mechanisms underlying the recovery of urinary bladder function following spinal cord injury. J. Auton. Nerv. Syst. 30, S71–S77 (Suppl.).

Erickson, J.D., Weihe, E., Schafer, M.K., Neale, E., Williamson, L., Bonner, T.I., Tao-Cheng, J.H., Eiden, L.E., 1996. The VAChT/ChAT "cholinergic gene locus": new aspects of genetic and vesicular regulation of cholinergic function. Prog. Brain Res. 109, 69–82.

Ferguson, S.M., Savchenko, V., Apparsundaram, S., Zwick, M., Wright, J., Heilman, C.J., Yi, H., Levey, A.I., Blakely, R.D., 2003. Vesicular localization and activity-dependent trafficking of presynaptic choline transporters. J. Neurosci. 23, 9697–9709.

Hoang, T.X., Pikov, V., Havton, L.A., 2006. Functional reinnervation of the rat lower urinary tract after cauda equina injury and repair. J. Neurosci. 26, 8672–8679.

Jacobsson, G., Piehl, F., Meister, B., 1998. VAMP-1 and VAMP-2 gene expression in rat spinal motoneurones: differential regulation after neuronal injury. Eur. J. Neurosci. 10, 301–316.

Keast, J.R., 1999. Unusual autonomic ganglia: connections, chemistry, and plasticity of pelvic ganglia. Int. Rev. Cytol. 193, 1–69.

Keast, J.R., 2004. Remodelling of connections in pelvic ganglia after hypogastric nerve crush. Neuroscience 126, 405–414.

Kepper, M.E., Keast, J.R., 1998. Specific targeting of ganglion cell sprouts provides an additional mechanism for restoring peripheral motor circuits in pelvic ganglia after spinal nerve damage. J. Neurosci. 18, 7987–7995.

Krenz, N.R., Weaver, L.C., 1998. Sprouting of primary afferent fibers after spinal cord transection in the rat. Neuroscience 85, 443–458.

Kruse, M.N., Belton, A.L., de Groat, W.C., 1993. Changes in bladder and external urethral sphincter function after spinal cord injury in the rat. Am. J. Physiol. 264, R1157–R1163.

Kruse, M.N., Bennett, B., De Groat, W.C., 1994. Effect of urinary diversion on the recovery of micturition reflexes after spinal cord injury in the rat. J. Urol. 151, 1088–1091.

Kruse, M.N., Bray, L.A., de Groat, W.C., 1995. Influence of spinal cord injury on the morphology of bladder afferent and efferent neurons. J. Auton. Nerv. Syst. 54, 215–224.

Maeda, M., Ohba, N., Nakagomi, S., Suzuki, Y., Kiryu-Seo, S., Namikawa, K., Kondoh, W., Tanaka, A., Kiyama, H., 2004. Vesicular acetylcholine transporter can be a morphological marker for the reinnervation to muscle of regenerating motor axons. Neurosci. Res. 48, 305–314.

Marson, L., 1997. Identification of central nervous system neurons that innervate the bladder body, bladder base, or external urethral sphincter of female rats: a transneuronal tracing study using pseudorabies virus. J. Comp. Neurol. 389, 584–602.

Marson, L., Gravitt, K., 2004. Spinal neurons activated with the urethrogenital reflex in the male rat. Brain Res. 1026, 108–115.

Matsuura, J., Ajiki, K., Ichikawa, T., Misawa, H., 1997. Changes of expression levels of choline acetyltransferase and vesicular acetylcholine transporter mRNAs after transection of the hypoglossal nerve in adult rats. Neurosci. Lett. 236, 95–98.

McKenna, K.E., Nadelhaft, I., 1986. The organization of the

pudendal nerve in the male and female rat. J. Comp. Neurol. 248, 532–549.
Nadelhaft, I., Booth, A.M., 1984. The location and morphology of preganglionic neurons and the distribution of visceral afferents from the rat pelvic nerve: a horseradish peroxidase study. J. Comp. Neurol. 226, 238–245.
Nadelhaft, I., Vera, P.L., 1996. Neurons in the rat brain and spinal cord labeled after pseudorabies virus injected into the external urethral sphincter. J. Comp. Neurol. 375, 502–517.
Piehl, F., Arvidsson, U., Johnson, H., Cullheim, S., Dagerlind, A., Ulfhake, B., Cao, Y., Elde, R., Pettersson, R.F., Terenius, L., et al., 1993. GAP-43, aFGF, CCK and alpha- and beta-CGRP in rat spinal motoneurons subjected to axotomy and/or dorsal root severance. Eur. J. Neurosci. 5, 1321–1333.
Pikov, V., Wrathall, J.R., 2001. Coordination of the bladder detrusor and the external urethral sphincter in a rat model of spinal cord injury: effect of injury severity. J. Neurosci. 21, 559–569.
Schafer, M.K., Weihe, E., Varoqui, H., Eiden, L.E., Erickson, J.D., 1994. Distribution of the vesicular acetylcholine transporter (VAChT) in the central and peripheral nervous systems of the rat. J. Mol. Neurosci. 5, 1–26.
Schafer, M.K., Eiden, L.E., Weihe, E., 1998. Cholinergic neurons and terminal fields revealed by immunohistochemistry for the vesicular acetylcholine transporter. II. The peripheral nervous system. Neuroscience 84, 361–376.
Schroder, H.D., 1980. Organization of the motoneurons innervating the pelvic muscles of the male rat. J. Comp. Neurol. 192, 567–587.
Seki, S., Sasaki, K., Fraser, M.O., Igawa, Y., Nishizawa, O., Chancellor, M.B., de Groat, W.C., Yoshimura, N., 2002. Immunoneutralization of nerve growth factor in lumbosacral spinal cord reduces bladder hyperreflexia in spinal cord injured rats. J. Urol. 168, 2269–2274.
Usdin, T.B., Eiden, L.E., Bonner, T.I., Erickson, J.D., 1995. Molecular biology of the vesicular ACh transporter. Trends Neurosci. 18, 218–224.
Vizzard, M.A., Erickson, V.L., Card, J.P., Roppolo, J.R., de Groat, W.C., 1995. Transneuronal labeling of neurons in the adult rat brainstem and spinal cord after injection of pseudorabies virus into the urethra. J. Comp. Neurol. 355, 629–640.
Weihe, E., Tao-Cheng, J.H., Schafer, M.K., Erickson, J.D., Eiden, L.E., 1996. Visualization of the vesicular acetylcholine transporter in cholinergic nerve terminals and its targeting to a specific population of small synaptic vesicles. Proc. Natl. Acad. Sci. U. S. A. 93, 3547–3552.
Wooten, G.F., Park, D.H., Joh, T.H., Reis, D.J., 1978. Immunochemical demonstration of reversible reduction in choline acetyltransferase concentration in rat hypoglossal nucleus after hypoglossal nerve transection. Nature 275, 324–325.
Yoshiyama, M., Nezu, F.M., Yokoyama, O., de Groat, W.C., Chancellor, M.B., 1999. Changes in micturition after spinal cord injury in conscious rats. Urology 54, 929–933.

THE JOURNAL OF BIOLOGICAL CHEMISTRY VOL. 282, NO. 32, pp. 23491–23499, August 10, 2007

Identification of Peripherin as a Akt Substrate in Neurons*

Received for publication, December 21, 2006, and in revised form, May 22, 2007 Published, JBC Papers in Press, June 14, 2007, DOI 10.1074/jbc.M611703200

Hiroyuki Konishi[‡], Kazuhiko Namikawa[‡§], Keiji Shikata[¶], Yuji Kobatake[‡], Taro Tachibana[¶], and Hiroshi Kiyama[‡1]

From the [‡]Department of Anatomy and Neurobiology, Osaka City University, Graduate School of Medicine, Osaka 545-8585, Japan, the [§]Department of Anatomy, Asahikawa Medical College, Asahikawa, Hokkaido 078-8510, Japan, and the [¶]Department of Bioengineering, Osaka City University, Graduate School of Engineering, Osaka 558-8585, Japan

Activation of Akt-mediated signaling pathways is crucial for survival and regeneration of injured neurons. In this study, we attempted to identify novel Akt substrates by using an antibody that recognized a consensus motif phosphorylated by Akt. PC12 cells that overexpressed constitutively active Akt were used. Using two-dimensional PAGE, we identified protein spots that exhibited increased immunostaining of the antibody. Mass spectrometry revealed several major spots as the neuronal intermediate filament protein, peripherin. Using several peripherin fragments, the phosphorylation site was determined as Ser[66] in its head domain *in vitro*. Furthermore, a co-immunoprecipitation experiment revealed that Akt interacted with the head domain of peripherin in HEK 293T cells. An antibody against phosphorylated peripherin was raised, and induction of phosphorylated peripherin was observed not only in Akt-activated cultured cells but also in nerve-injured hypoglossal motor neurons. These results suggest that peripherin is a novel substrate for Akt *in vivo* and that its phosphorylation may play a role in motor nerve regeneration.

Akt (also known as protein kinase B) is a Ser/Thr kinase that plays essential roles in various cellular processes such as cell survival, proliferation, and differentiation (1). In the nervous system, Akt is suggested to be involved in neurogenesis (2, 3), neuronal survival (4), axon or dendrite formation (5, 6), synaptogenesis (7, 8), and synaptic transmission (9). The most evident role of all may be its neuroprotective action. For instance, several previous papers have demonstrated a strong protective effect of Akt on damaged neurons *in vivo* (10–13). Of particular interest, Akt was proven to have a crucial role in neuronal survival after peripheral nerve injury (10). In the peripheral nervous system, in which most neurons can survive and regenerate after injury, glial cells secrete various trophic factors to promote survival and regeneration of nerve-injured neurons. Astrocytes and microglia, which are located around the neuronal cell bodies, are thought to secrete various factors toward injured neurons (14, 15). Furthermore, in the distal stump of axons far from neuronal cell bodies, Schwann cells also secrete trophic factors (16). Such factors released from those glial cells include a wide range of growth factors such as nerve growth factor, brain-derived neurotrophic factor, glial cell line-derived neurotrophic factor, and fibroblast growth factor-2 (17–19). They are known to activate the phosphatidylinositol 3-kinase-Akt pathway in injured neurons via their respective receptors (20–22). In fact, our previous study showed that Akt activity was markedly induced in motor neurons after nerve injury (10). We also revealed that activated Akt accelerated axonal elongation, as well as neuronal survival. It is well established that activated Akt exerts its function by phosphorylating its substrates; however, the substrates that specifically exist in neurons are largely unidentified. Thus, identification of novel neuronal substrates is pivotal to gain further insight into the function of Akt in neuronal regeneration.

In this study, we attempted to identify novel Akt substrates in neurons by a proteomic approach, using a unique antibody that recognizes the consensus motif phosphorylated by Akt. Here we demonstrate that peripherin, which is a peripheral nervous system neuron-specific intermediate filament protein, is a novel Akt substrate, and that Ser[66] of peripherin is the phosphorylation site. Peripherin phosphorylation is apparently induced in motor neurons after nerve injury, suggesting that the Akt-mediated peripherin phosphorylation may play a role in motor nerve regeneration.

EXPERIMENTAL PROCEDURES

Materials—Anti-phospho-Akt substrate antibody (antibody 9611; Cell Signaling Technology, Danvers, MA), anti-phospho-Akt antibody (antibody 4051; Cell Signaling Technology), anti-peripherin antibody (antibody MAB1527 for Western blotting; antibody AB1530 for immunohistochemistry; Chemicon, Temecula, CA), anti-glutathione *S*-transferase (GST)[2] antibody (antibody sc-138; Santa Cruz Biotechnology, Santa Cruz, CA), anti-His antibody (antibody 1922416; Roche Applied Science), anti-hemagglutinin (HA) antibody (antibody 1583816; Roche Applied Science; and antibody sc-138; Santa Cruz Biotechnology), anti-FLAG antibody (antibody F3166; Sigma), and anti-glyceraldehydes-3-phosphate dehydrogenase (antibody 4300; Ambion, Huntington, UK) were used as primary antibod-

* This work was supported in part by grants from the Ministry of Health, Labor and Welfare of Japan, the Ministry of Education, Culture, Sports, Science, and Technology, and the General Insurance Association of Japan. The costs of publication of this article were defrayed in part by the payment of page charges. This article must therefore be hereby marked "*advertisement*" in accordance with 18 U.S.C. Section 1734 solely to indicate this fact.

[1] To whom correspondence should be addressed: Dept. of Anatomy and Neurobiology, Osaka City University, Graduate School of Medicine, 1-4-3 Abeno-ku, Asahimachi, Osaka 545-8585, Japan. Tel.: 81-6-6645-3701; Fax: 81-6-6645-3702; E-mail: kiyama@med.osaka-cu.ac.jp.

[2] The abbreviations used are: GST, glutathione *S*-transferase; HA, hemagglutinin; HEK, human embryonic kidney; WT, wild type; CA, constitutively active; DN, dominant negative; MOI, multiplicity of infection; MALDI-TOF, matrix-assisted laser desorption/ionization time of flight; p70S6K, p70 S6 kinase; NF, neurofilament; CHAPS, 3-[(3-cholamidopropyl)dimethylammonio]-1-propanesulfonic acid; PBS, phosphate-buffered saline; GAPDH, glyceraldehyde-3-phosphate dehydrogenase.

ies. As secondary antibodies, horseradish peroxidase-conjugated antibodies (Amersham Biosciences) and Alexa Fluor-conjugated antibodies (Molecular Probes, Eugene, OR) were used for Western blotting and immunohistochemistry, respectively. All of the inhibitors were obtained from Calbiochem (La Jolla, CA).

Cell Culture—Human embryonic kidney (HEK) 293T cells were maintained in Dulbecco's modified Eagle's medium containing 10% fetal bovine serum (Invitrogen) and 0.05 mg/ml penicillin/streptomycin (Invitrogen). PC12 cells were maintained on cell culture dishes coated with collagen in RPMI 1640 containing 5% fetal bovine serum, 10% horse serum, and 0.05 mg/ml penicillin/streptomycin. Both cell types were cultured at 37 °C under 5% CO_2.

Adenoviral Vectors—The detailed procedure for constructing recombinant adenoviral vectors was described previously (10). Briefly, HA-tagged wild type Akt (HA-WT-Akt), constitutively active Akt (HA-CA-Akt), which lacks its pleckstrin homology domain but has a Src myristoylation signal sequence, and dominant negative Akt (T308A/S473A; HA-DN-Akt; kindly provided by Drs. M. Kasuga and W. Ogawa) were subcloned into pAxCALNLw Cre-lox P system-mediated expression cassette (23–25). The adenoviral vectors AxCALNLHA-WT-Akt, AxCALNLHA-CA-Akt, and AxCALNLHA-DN-Akt were then constructed by the COS-terminal protein complex method (26). AxCANCre and AxCALNLLacZ were kindly provided by Drs. I. Saito and Y. Kanegae (27).

Two-dimensional PAGE—PC12 cells grown on 10-cm cell culture dishes were infected with AxCALNLLacZ (multiplicity of infection (MOI) 100) or AxCALNLHA-CA-Akt (MOI 100) together with AxCANCre (MOI 30). The cells were collected 48 h after infection, washed once with PBS, and lysed in a buffer containing 40 mM Tris base, 8 M urea, and 2% CHAPS. After centrifugation at 10,000 × *g* for 20 min at 4 °C, the supernatants were aliquoted and stored at −80 °C until use. Two-dimensional PAGE was performed according to the previous report with slight modification (28). Immobiline DryStrips (pH 3–10, 7 cm; pH 4.5–5.5, 24 cm; Amersham Biosciences) were rehydrated with rehydration solution containing 60 μg (for 7 cm gel) or 240 μg (for 24 cm gel) of the supernatants, 8 M urea, 2% CHAPS, 0.5% IPG buffer (Amersham Biosciences), 20 mM dithiothreitol, and bromphenol blue for 12 h at 20 °C. Isoelectric focusing was then performed using the IPGphor Isoelectric Focusing System (Amersham Biosciences) (500 V for 1 h, 1000 V for 1 h, and 8000 V for 2–3 h at 20 °C). The strips were equilibrated with a buffer containing Tris-HCl, pH 6.8, 6 M urea, 30% glycerol, 2% SDS, and 65 mM dithiothreitol for 20 min at room temperature, fixed vertically on top of the SDS-polyacrylamide gel by 1.5% agarose in running buffer, and subjected to 25 mA/gel in a cold room. The gels were analyzed by Western blotting for immunostaining or SYPRO Ruby for protein staining according to the manufacturer's protocol (Molecular Probes, Eugene, OR).

In-gel Digestion—Protein spots were punched out from the gel, trimmed into small pieces, destained in a solution containing 50% acetonitrile and 25 mM NH_4HCO_3, and dehydrated. The gel pieces were then rehydrated in a solution containing 10 mM dithiothreitol and 25 mM NH_4HCO_3 and subsequently treated with 25 mM NH_4HCO_3 containing 55 mM iodoacetoamide. Following the dehydration step, gel pieces were rehydrated in trypsin solution containing 10 mg/ml trypsin and 25 mM NH_4HCO_3 overnight at 37 °C, and finally digested peptides were eluted with 50% acetonitrile containing 5% trifluoroacetic acid.

Mass Spectrometry—The eluate containing digested peptides was desalted with ZipTip (Millipore, Bedford, MA). The solution was then mixed with an equal volume of saturated α-cyano-4-hydroxycinnamic acid solution dissolved in 30% acetonitrile and 0.1% trifluoroacetic acid and spotted onto a target plate. Mass spectrometry was performed on a matrix-assisted laser desorption/ionization time of flight (MALDI-TOF) mass spectrometer Reflex III (Bruker Daltonics, Billerica, MA) with reflector mode. Obtained peptide mass fingerprinting data were searched against the NCBI data base using the MASCOT search engine (Matrix Science, Boston, MA).

Western Blotting—Protein extracts were separated by SDS-PAGE, and blots were prepared on polyvinylidene difluoride membranes (Millipore). For two-dimensional gels, whole 7-cm gels or part of 24-cm gels were prepared on the membrane. The blots were probed with primary and subsequent secondary antibodies and visualized by using the chemiluminescence system (Western Lightning; PerkinElmer Life Sciences). If necessary, the membranes were stripped of antibodies by incubating in stripping buffer containing 62.5 mM Tris-HCl, pH 6.8, 2% SDS, and 100 mM 2-mercaptoethanol for 30 min at 50 °C and then probed with another antibody.

Preparation of Recombinant Proteins—To generate GST fusion proteins, partial sequences for 1–60, 51–100, 181–251, and 301–350 amino acids of peripherin were amplified from full-length mouse peripherin cDNA (kindly provided by Dr. F. Landon) and subcloned into pGEX 5X-1 (Amersham Biosciences). Site-directed mutagenesis (Ser^{66} or Ser^{79} to Ala) was introduced by PCR primers carrying these mutations. BL21 bacteria transformed with these vectors were stimulated with 0.2 mM isopropyl-β-D-thiogalactopyranoside overnight at 20 °C, harvested by brief centrifugation, and lysed in PBS containing 1% Triton X-100 for 30 min at 4 °C. The supernatants were subsequently incubated with glutathione-Sepharose 4B (Amersham Biosciences) for 1 h at 4 °C, and the bound proteins were eluted by adding 10 mM reduced glutathione in 50 mM Tris-HCl, pH 8.0. After removal of glutathione by dialysis against PBS, the proteins were checked by SDS-PAGE followed by Coomassie Brilliant Blue R-250 staining and stored at −80 °C until use.

In Vitro Kinase Assay—2.5 μg of GST fusion proteins were incubated with or without 100 ng of recombinant His-tagged CA-Akt (His-CA-Akt) (Upstate Biotechnology) in 20 mM Tris-HCl, pH 7.5, 10 mM $MgCl_2$, 20 μM ATP, and 30 kBq [γ-^{32}P]ATP (PerkinElmer Life Sciences) for 30 min at 30 °C. The reaction mixtures were subjected to SDS-PAGE, and phosphorylation of the fragments was detected by autoradiography. For Western blot analysis, 1 μg of GST fusion proteins was reacted with 100 ng of His-CA-Akt, and one-tenth of the reaction mixtures was analyzed.

Phosphorylation-specific Antibody—A rat monoclonal antibody that specifically recognized phosphorylated peripherin